Supplement of Atmos. Chem. Phys., 26, 4019–4047, 2026
https://doi.org/10.5194/acp-26-4019-2026-supplement

Atmospheric Chemistry and Physics
Open Access
EGU

Supplement of

Regional and seasonal distribution of Arctic low-level cloud types and their relationship to large-scale environmental conditions

Aymeric Dziduch et al.

Correspondence to: Olivier Jourdan (olivier.jourdan@uca.fr)

Class number	Definition
-2	Presence of liquid unknown
-1	Surface and subsurface
0	Clear sky
1	Ice clouds
2	Spherical or 2D ice
3	Supercooled water
4	Supercooled water + ice
5	Cold rain
6	Aerosols
7	Warm rain
8	Stratospheric clouds
9	Highly concentrated ice
10	Top of convective towers
11	Liquid clouds
12	Warm rain + liquid clouds
13	Cold rain + liquid clouds
14	Rain may be mixed with liquid
15	Multiple scattering due to supercooled water

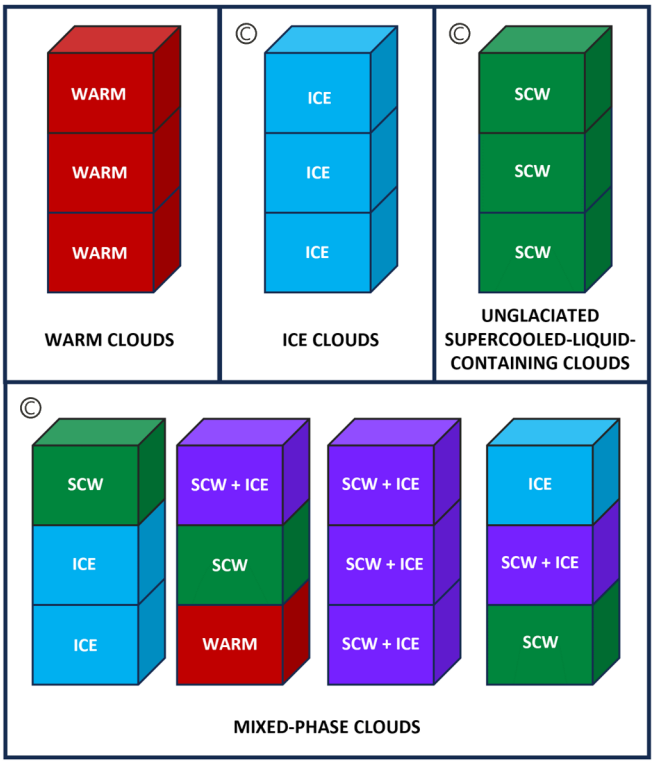

Figure S1. DARDAR classes used in the version V2.23 and cloud representation examples in DARDAR-SOCP (adapted from Bazantay et al., 2024). The colors of the classes in the table correspond to the pixel colors of the cloud representations. The symbol C in the diagrams represents cloud types belonging to the cold clouds (temperature < 0 °C).

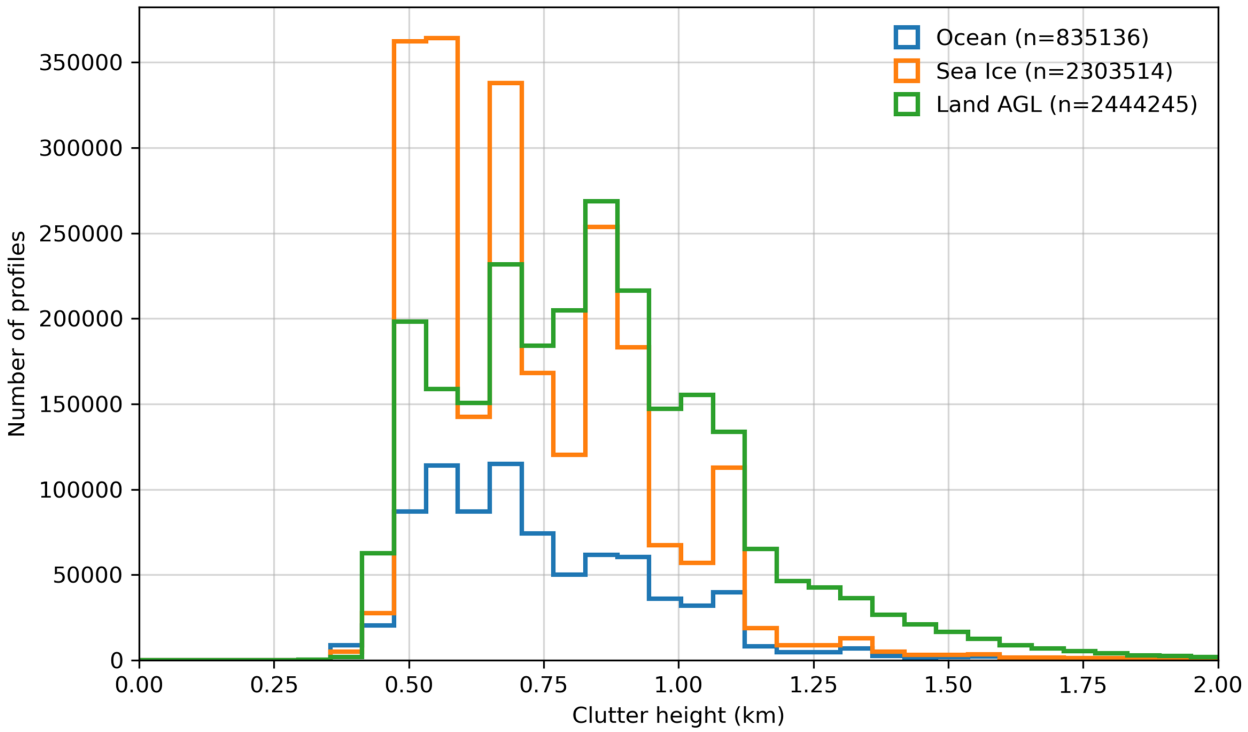

Figure S2. Distribution of CloudSat radar clutter height over ocean (blue), sea ice (orange), and land (green). The value of n indicates the number of profiles for each surface type.

Table S1. Mean and median values of clutter height for different surfaces: ocean, sea ice and land (above ground level)

Surface type	Mean (m)	Median (m)
Ocean	810	660
Sea Ice	783	660
Land (above ground level)	901	833

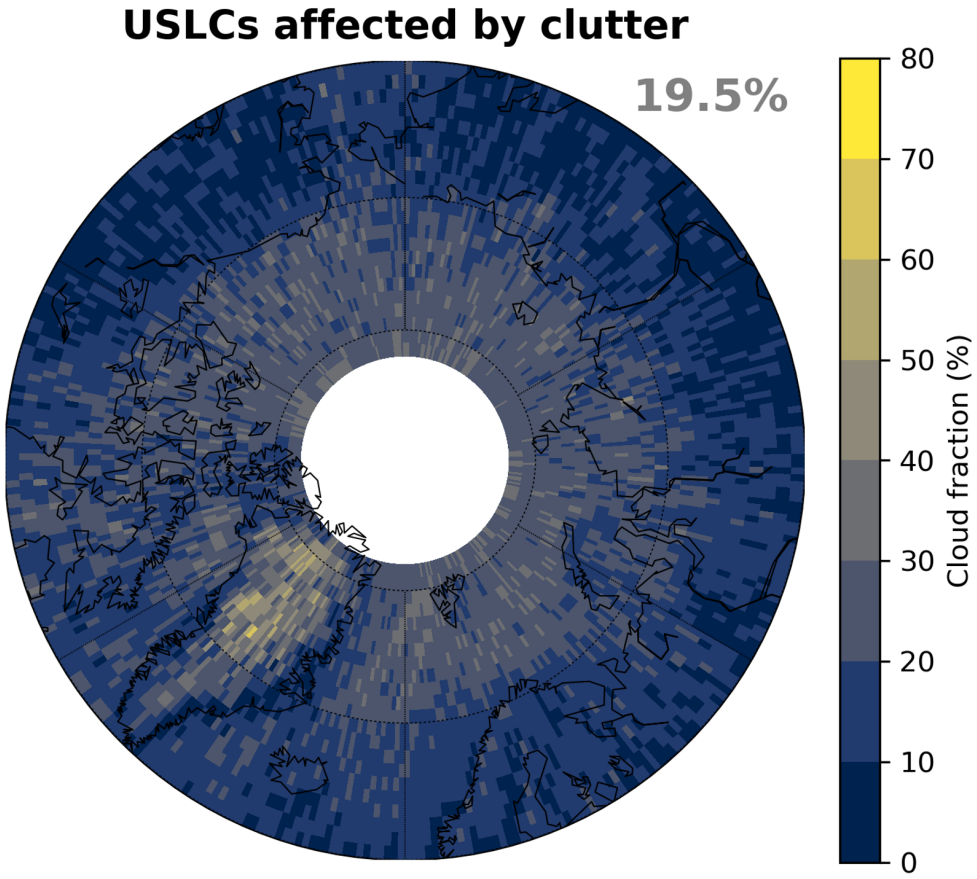

Figure S3. Fraction of USLCs affected by clutter over 8 years of measurement (2007-2016)

Table S2. Averages and standard deviations (σ) of the differences between ground-based and space-based cloud occurrences for Ny Ålesund (Norway, 78.923°N, 11.922°E), Hyytiälä Hyytiälä (Finland, 61.844°N, 24.287°E), and both sites combined.

		Cloud type					
Site		Total	Warm	Cold	Ice	MPC	CLCC
Ny-Ålesund	Average	0.3	1.3	-2.1	5.2	0.1	-5.8
	σ	16.5	4.5	16.0	23.6	9.4	7.6
Hyytiälä	Average	0.2	5.3	-1.7	-2.9	3.4	-2.3
	σ	8.4	5.5	10.8	8.1	7.1	8.2
Total	Average	0.2	3.3	-1.9	1.1	1.7	-4.0
	σ	12.6	5.2	13.1	17.5	8.2	7.8

a)

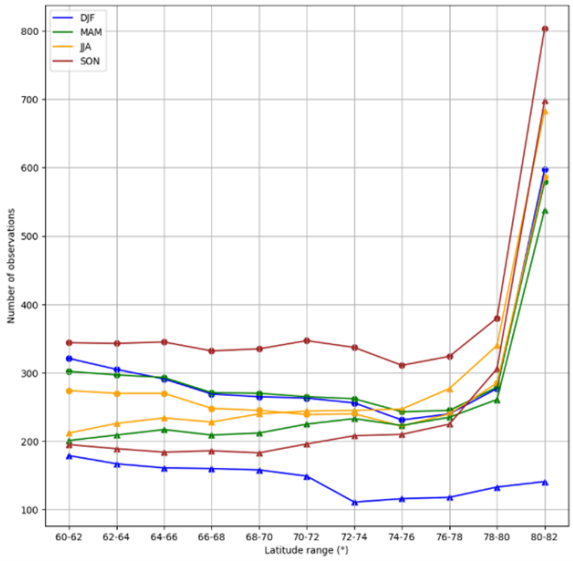

b)

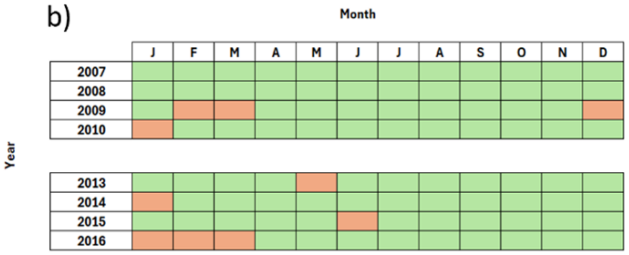

c)

	2007-2010		2013-2016	
	Total clouds	MPCs	Total clouds	MPCs
All seasons	51,39	18,87	51,44	17,72
DJF	42,29	12,89	43,71	12,63
MAM	47,11	15,78	49,06	16,41
JJA	46,58	18,58	48,04	17,72
SON	64,95	25,93	64,95	23,55

Figure S4. **(a)** Average number of observations per grid cell as a function of latitude for the 4 seasons (winter in blue, spring in green, summer in yellow, and autumn in brown). The circles represent the 2007-2010 period and the triangles the 2013-2016 period. Table **(b)** represents the availability of DARDAR mask v2.23 data for this study (green: available and orange: not available). Table **(c)** compares the average low-level cloud occurrences (between 500 and 3000 m above sea level) for the seasons between the 2 periods (2007-2010 and 2013-2016) for total clouds and MPCs.

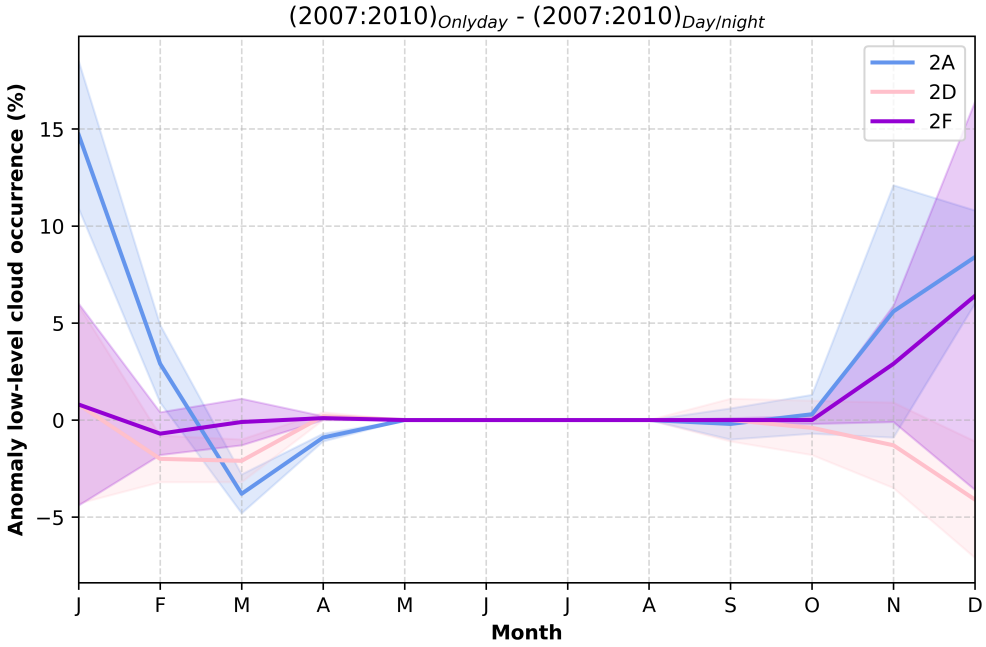

Figure S5. Low-level cloud (between 500 and 3000 m above sea level) anomalies for 3 high-latitude regions (2A, 2D, and 2F) for the period 2007-2010 with two operating modes: day only and day/night. The colored curves represent the average values and the colored areas around the curves represent the standard deviation range.

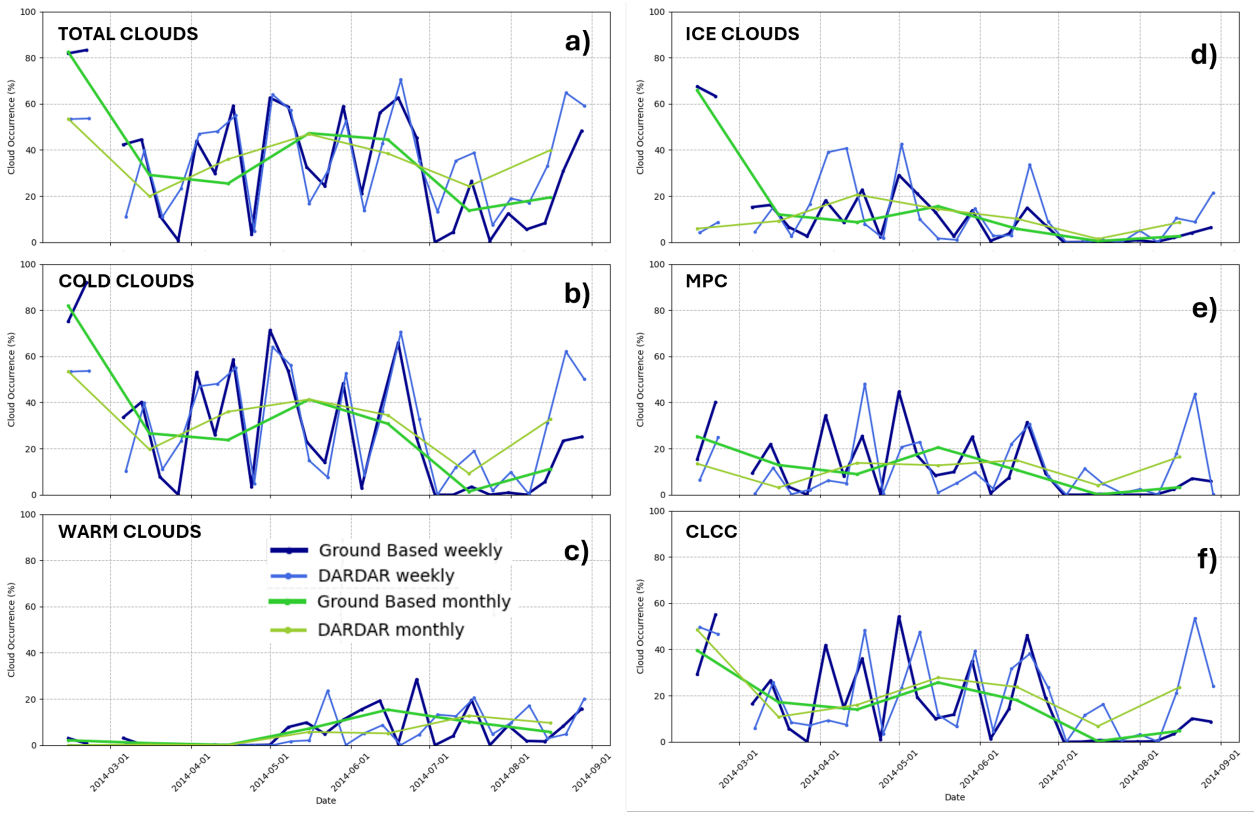

Figure S6. Comparison of DARDAR and ground-based observations of : **(a)** total, **(b)** cold, **(c)** warm, **(d)** ice, **(e)** mixed-phase, and **(f)** cold liquid-containing cloud occurrence up to 3000 m above ground level at Hyytiälä (Finland, 61.84°N, 24.28°E). Weekly (blue) and monthly (green) occurrences are shown. Ground-based observations are represented by thicker, darker lines.

a.

	SST	Surf_Temp	Surf_Pres	IWV	Temp_850hPa	Temp_700hPa	MCAO	LTS	EIS	SH_850hPa	SH_700hPa	GH_850hPa	GH_700hPa	Wind_Surf	Wind_850hPa	Wind_700hPa	SIC
MPCs	1,4	1,2	1,7	1,7	1,1	1,2	3,6	2,2	5,6	1,1	1,1	1,5	2,1	1,1	1,1	1,1	1,5
USCLs	1,1	1,1	1,6	1,3	1,3	1,3	1,9	1,3	1,1	1,5	1,6	1,5	1,2	1,2	1,3	1,1	1,0
Ice Clouds	1,7	2,1	1,1	1,2	12,1	7,9	1,3	1,3	1,2	1,2	1,4	1,3	1,3	1,2	1,2	1,0	1,1
Warm Clouds	2,8	2,5	1,2	1,1	7,8	6,1	1,5	1,1	1,7	2,9	2,5	1,1	2,1	1,0	1,0	1,1	1,4

Variance Inflation Factor (VIF)

b.

MPCs	0,26	0,,16	0,38	0,41	-0,1	-0,2	-0,56	-0,58	-0,35	-0,1	-0,1	-0,3	-0,5	-0,02	-0,1	-0,1	-0,3
USCLs	-0,1	-0,1	0,37	0,25	-0,2	-0,2	-0,2	-0,2	-0,3	-0,3	-0,4	-0,2	-0,3	-0,07	-0,1	-0,1	-0,07
Ice Clouds	-0,51	-0,49	-0,12	0,08	-0,59	-0,68	-0,1	-0,2	0,18	-0,6	-0,6	-0,7	-0,4	-0,02	0,02	0,5	0,28
Warm Clouds	0,59	0,62	0,2	0,15	0,65	0,68	0,12	-0,08	-0,38	0,67	0,59	0,48	0,08	-0,08	-0,02	-0,4	0,06

Spearman's rank correlations

Figure S7. **(a)** Variance Inflation Factor (VIF) computed for each explanatory variable and cloud type. Values exceeding the threshold of 10 indicate strong multicollinearity. **(b)** Spearman's rank correlations between cloud-type occurrences and environmental parameters.

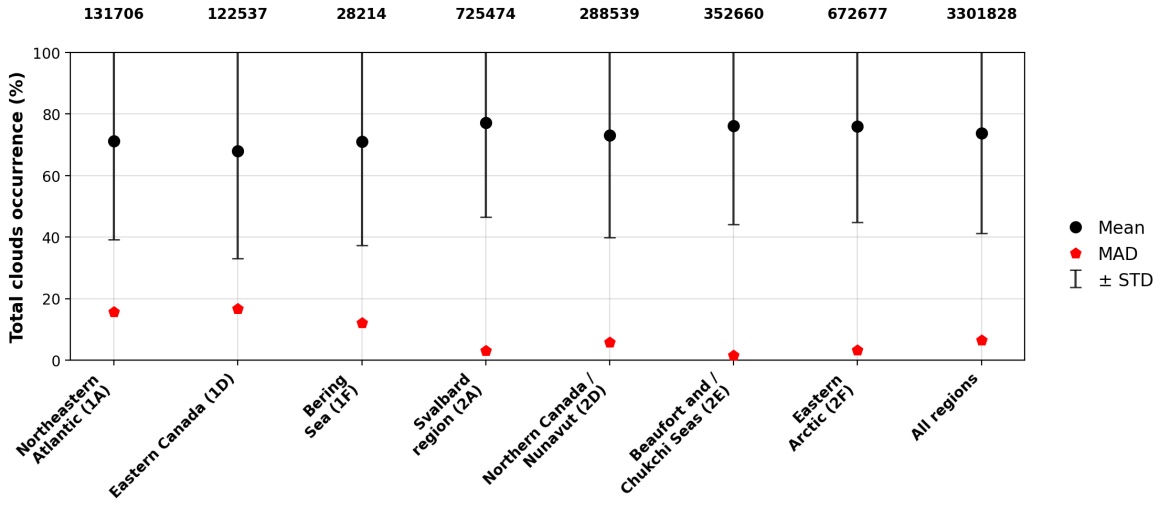

Figure S8. Statistical analysis of total low-level cloud occurrence (between the radar clutter height and 3000 m above ground level) derived from the DARDAR-MASK and DARDAR-SOCP products across different Arctic regions. Black circles indicate the mean occurrence with standard deviation, while red pentagons represent the median absolute deviation (MAD). The numbers above each boxplot denote the number of data points for each region.

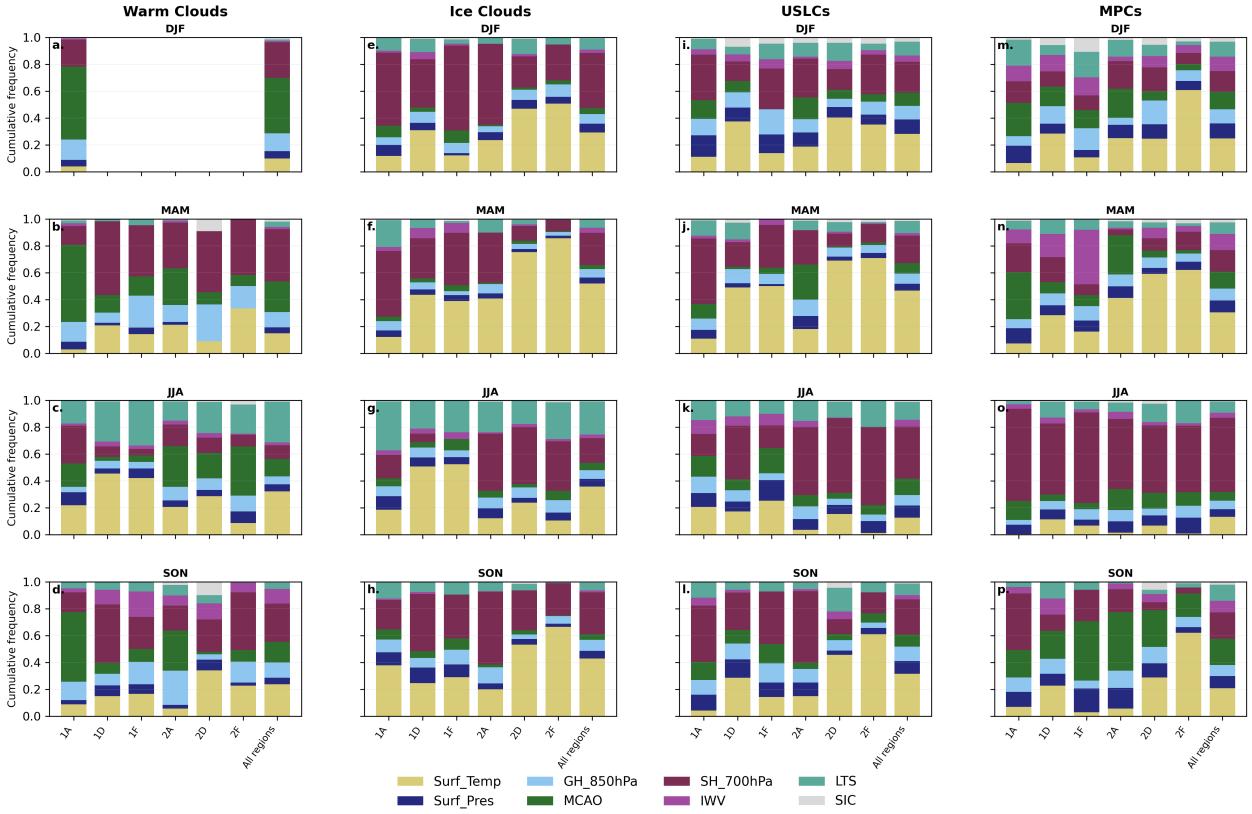

Figure S9. Cumulative frequency of most influential parameters of MLR for low-level (between clutter height and 3000 m above ground level) **(a-d)** warm clouds, **(e-h)** ice clouds, **(i-l)** USLCs, and **(m-p)** MPCs. Each row corresponds to a season. The most influential parameter is only selected when MLR has $R^2 > 0.1$.

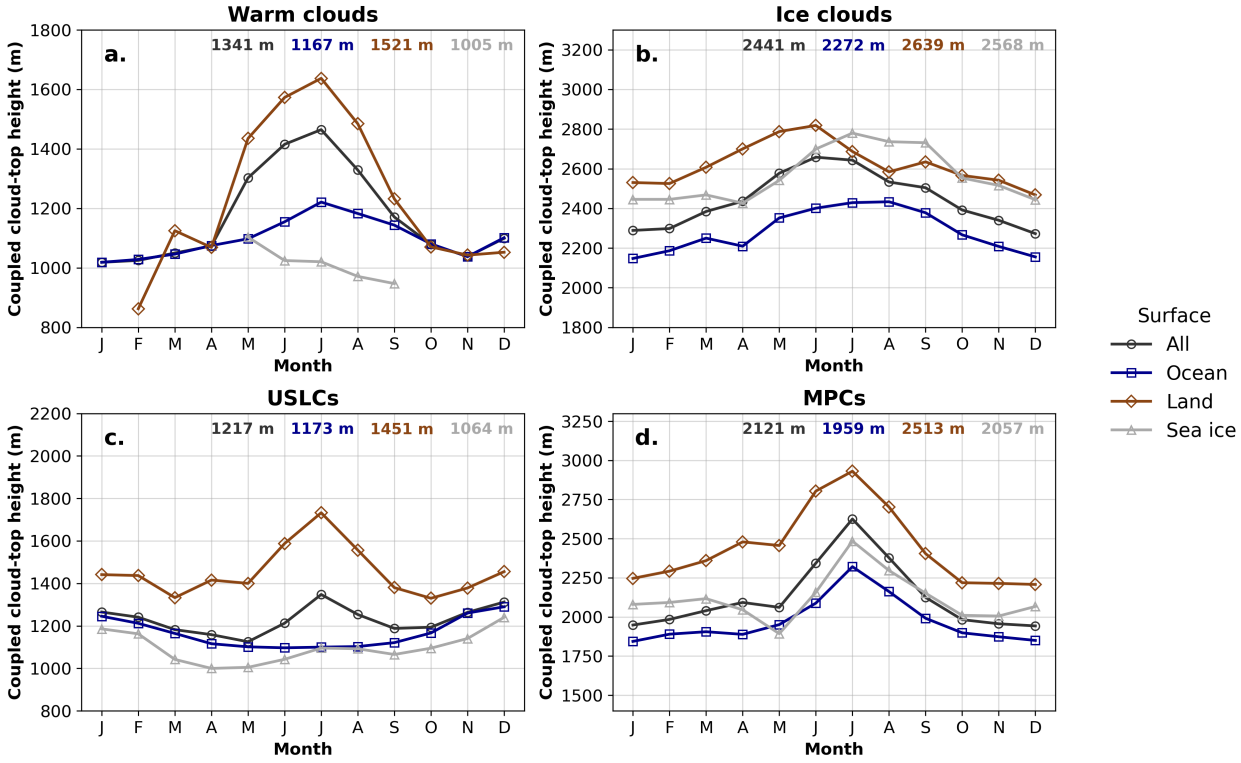

Figure S10. Monthly variations of the cloud-top height (m) for low-level coupled (between clutter-height and 3000 m above ground level) **(a)** warm clouds, **(b)** ice clouds, **(c)** USLCs, and **(d)** MPCs. Results are averaged over 2007–2016 and shown separately for different surface types: ocean (blue), land (brown), sea ice (grey), and all surfaces combined (black).

MPCs

Season	Region	SIC Slope	SIC Std error	SIC R^2	LTS Slope	LTS Std error	LTS R^2	Surf_Temp Slope	Surf_Temp Std error	Surf_Temp R^2
DJF	2A	-0,06	0,01	-0,74	-0,38	0,07	-0,65	0,65	0,05	0,88
	2D	0,00	0,04	-0,04	-0,28	0,06	-0,56	0,44	0,04	0,88
	2E	-0,21	0,05	-0,59	-0,48	0,07	-0,76	0,46	0,08	0,70
	2F	-0,09	0,02	-0,52	-0,58	0,08	-0,77	0,60	0,06	0,87
	All regions	-0,08	0,01	-0,79	-0,45	0,05	-0,85	0,58	0,06	0,79
MAM	2A	-0,07	0,01	-0,69	-0,59	0,10	-0,63	0,85	0,05	0,96
	2D	-0,08	0,03	-0,38	-1,02	0,07	-0,93	0,60	0,04	0,89
	2E	-0,04	0,05	-0,16	-1,29	0,11	-0,89	0,57	0,05	0,84
	2F	0,01	0,02	0,03	-1,09	0,07	-0,94	0,71	0,04	0,96
	All regions	-0,06	0,01	-0,79	-0,53	0,08	-0,71	0,52	0,04	0,92
JJA	2A	-0,02	0,01	-0,48	-0,89	0,13	-0,69	0,20	0,24	0,14
	2D	0,00	0,01	0,04	-0,05	0,11	-0,08	0,09	0,11	0,12
	2E	-0,01	0,01	-0,30	-0,60	0,12	-0,63	-0,06	0,18	-0,09
	2F	-0,02	0,01	-0,24	-0,71	0,13	-0,67	0,24	0,26	0,15
	All regions	-0,02	0,00	-0,63	-0,24	0,09	-0,41	-0,10	0,10	-0,14
SON	2A	-0,07	0,01	-0,68	-0,73	0,08	-0,80	0,52	0,05	0,85
	2D	-0,03	0,02	-0,27	-0,89	0,08	-0,90	0,33	0,06	0,61
	2E	-0,02	0,02	-0,12	-0,91	0,12	-0,72	0,33	0,09	0,45
	2F	-0,05	0,01	-0,65	-1,79	0,08	-0,98	0,44	0,11	0,51
	All regions	-0,05	0,01	-0,73	-0,82	0,07	-0,83	0,55	0,05	0,90
ALL	2A	-0,05	0,01	-0,85	-0,50	0,07	-0,70	0,53	0,06	0,82
	2D	-0,03	0,01	-0,46	-0,77	0,04	-0,99	0,26	0,04	0,67
	2E	-0,04	0,01	-0,60	-0,66	0,10	-0,69	0,24	0,07	0,50
	2F	-0,06	0,01	-0,80	-1,33	0,07	-0,91	0,44	0,05	0,74
	All regions	-0,05	0,00	-0,92	-0,49	0,07	-0,70	0,19	0,05	0,44

USLCs

Season	Region	SIC Slope	SIC Std error	SIC R^2	LTS Slope	LTS Std error	LTS R^2	Surf_Temp Slope	Surf_Temp Std error	Surf_Temp R^2
DJF	2A	-0,07	0,01	-0,80	-0,17	0,05	-0,46	0,55	0,02	0,92
	2D	-0,06	0,03	-0,26	-0,24	0,06	-0,48	0,61	0,03	0,92
	2E	-0,11	0,06	-0,38	-0,27	0,09	-0,41	0,48	0,06	0,77
	2F	-0,15	0,03	-0,58	-0,62	0,08	-0,72	0,52	0,04	0,90
	All regions	-0,07	0,01	-0,76	-0,11	0,05	-0,33	0,35	0,02	0,95
MAM	2A	-0,04	0,01	-0,77	-0,13	0,07	-0,28	0,76	0,03	0,98
	2D	-0,05	0,03	-0,26	-0,37	0,07	-0,63	0,61	0,06	0,86
	2E	-0,07	0,06	-0,21	-0,62	0,10	-0,67	0,77	0,06	0,88
	2F	-0,06	0,02	-0,36	-0,58	0,07	-0,80	0,77	0,04	0,94
	All regions	-0,03	0,01	-0,55	-0,18	0,06	-0,46	0,40	0,04	0,83
JJA	2A	-0,01	0,01	-0,18	-0,42	0,10	-0,48	-0,71	0,22	-0,52
	2D	-0,01	0,01	-0,15	-0,06	0,10	-0,07	-0,70	0,09	-0,74
	2E	-0,05	0,01	-0,53	-0,38	0,13	-0,42	-1,00	0,16	-0,81
	2F	0,00	0,01	-0,13	-0,38	0,13	-0,47	-0,94	0,18	-0,69
	All regions	0,00	0,00	-0,29	-0,01	0,10	-0,06	-0,42	0,07	-0,61
SON	2A	-0,04	0,01	-0,50	-0,26	0,04	-0,63	0,35	0,04	0,83
	2D	-0,04	0,01	-0,46	-0,27	0,07	-0,51	0,44	0,05	0,83
	2E	-0,04	0,01	-0,38	-0,17	0,06	-0,42	0,27	0,05	0,60
	2F	-0,05	0,01	-0,74	0,18	0,07	0,32	0,17	0,08	0,34
	All regions	-0,05	0,00	-0,84	-0,10	0,06	-0,23	0,42	0,03	0,83
ALL	2A	-0,04	0,00	-0,83	-0,17	0,05	-0,53	0,39	0,04	0,81
	2D	-0,04	0,01	-0,55	-0,32	0,04	-0,78	0,17	0,04	0,52
	2E	-0,05	0,01	-0,60	-0,27	0,07	-0,48	0,13	0,07	0,28
	2F	-0,04	0,01	-0,70	-0,36	0,06	-0,66	0,34	0,05	0,69
	All regions	-0,04	0,00	-0,89	-0,11	0,06	-0,36	0,10	0,04	0,26

P-value
> 0,05
< 0,05 & > 0,01
< 0,01

Ice Clouds

Season	Region	SIC Slope	SIC Std error	SIC R^2	LTS Slope	LTS Std error	LTS R^2	Surf_Temp Slope	Surf_Temp Std error	Surf_Temp R^2
DJF	2A	-0,02	0,01	-0,30	-0,54	0,10	-0,58	0,21	0,05	-0,53
	2D	-0,03	0,07	-0,05	-0,16	0,09	-0,28	-0,14	0,08	-0,28
	2E	0,06	0,07	0,12	-0,16	0,11	-0,25	-0,02	0,07	-0,07
	2F	0,05	0,03	0,23	-0,14	0,10	-0,18	-0,01	0,08	-0,03
	All regions	-0,02	0,01	-0,22	-0,52	0,06	-0,82	0,24	0,05	-0,63
MAM	2A	0,01	0,01	0,16	-0,42	0,07	-0,69	-0,15	0,06	-0,36
	2D	0,05	0,03	0,23	-0,42	0,09	-0,60	-0,23	0,07	-0,42
	2E	0,08	0,06	0,20	-0,30	0,09	-0,44	0,00	0,08	-0,03
	2F	0,01	0,03	0,01	0,11	0,08	0,16	-0,17	0,06	-0,43
	All regions	0,00	0,01	-0,23	-0,42	0,05	-0,81	-0,11	0,05	-0,34
JJA	2A	0,01	0,01	-0,01	-1,33	0,07	-0,91	-1,18	0,16	-0,74
	2D	-0,02	0,01	-0,12	-0,69	0,16	-0,58	-0,90	0,12	-0,79
	2E	0,02	0,01	0,14	-1,07	0,11	-0,86	-1,37	0,14	-0,88
	2F	0,03	0,01	0,27	-0,95	0,14	-0,74	-0,85	0,26	-0,44
	All regions	0,01	0,00	0,35	-0,70	0,12	-0,68	-0,59	0,06	-0,78
SON	2A	0,01	0,01	0,16	0,01	0,09	-0,02	-0,29	0,10	-0,37
	2D	0,04	0,02	0,21	-0,17	0,12	-0,21	-0,07	0,09	-0,12
	2E	0,03	0,02	0,23	-0,11	0,10	-0,14	0,05	0,08	0,06
	2F	0,02	0,01	0,16	0,05	0,12	0,00	0,04	0,10	0,07
	All regions	0,01	0,01	0,25	0,00	0,11	0,03	-0,12	0,06	-0,28
ALL	2A	0,01	0,01	-0,01	-0,52	0,08	-0,62	-0,18	0,07	-0,37
	2D	0,00	0,01	0,04	-0,45	0,06	-0,72	-0,35	0,04	-0,81
	2E	0,01	0,01	0,12	-0,33	0,08	-0,51	-0,27	0,07	-0,47
	2F	0,01	0,01	0,25	-0,23	0,06	-0,46	-0,18	0,07	-0,39
	All regions	0,02	0,00	0,13	-0,49	0,05	-0,88	-0,34	0,04	-0,78

Total Clouds

Season	Region	SIC Slope	SIC Std error	SIC R^2	LTS Slope	LTS Std error	LTS R^2	Surf_Temp Slope	Surf_Temp Std error	Surf_Temp R^2
DJF	2A	-0,16	0,01	-0,88	-1,23	0,06	-0,95	1,19	0,08	0,87
	2D	0,02	0,07	-0,01	-0,85	0,10	-0,78	0,78	0,08	0,86
	2E	-0,20	0,07	-0,46	-0,87	0,12	-0,79	0,53	0,12	0,53
	2F	-0,20	0,05	-0,49	-1,42	0,10	-0,94	0,93	0,10	0,80
	All regions	-0,18	0,02	-0,83	-1,19	0,06	-0,91	0,97	0,05	0,96
MAM	2A	-0,12	0,01	-0,83	-1,43	0,07	-0,92	1,16	0,07	0,96
	2D	-0,08	0,05	-0,24	-1,39	0,07	-0,91	0,74	0,09	0,74
	2E	0,03	0,08	0,03	-2,15	0,10	-0,93	1,00	0,11	0,80
	2F	-0,01	0,03	-0,05	-1,49	0,11	-0,87	1,07	0,09	0,84
	All regions	-0,09	0,01	-0,80	-1,15	0,07	-0,98	0,54	0,08	0,72
JJA	2A	-0,03	0,01	-0,36	-2,18	0,11	-0,99	-0,84	0,46	-0,25
	2D	-0,02	0,02	-0,19	-1,04	0,32	-0,50	-1,59	0,17	-0,82
	2E	-0,04	0,01	-0,38	-2,05	0,17	-0,85	-1,83	0,31	-0,78
	2F	-0,01	0,01	-0,13	-1,59	0,23	-0,75	-1,31	0,34	-0,56
	All regions	-0,01	0,01	-0,16	-0,64	0,24	-0,36	-0,99	0,15	-0,71
SON	2A	-0,10	0,01	-0,71	-1,03	0,12	-0,83	0,60	0,11	0,64
	2D	-0,04	0,02	-0,27	-1,38	0,12	-0,85	0,62	0,13	0,61
	2E	-0,05	0,02	-0,31	-1,35	0,15	-0,76	0,43	0,18	0,31
	2F	-0,11	0,01	-0,90	-1,84	0,13	-0,90	0,98	0,14	0,69
	All regions	-0,09	0,01	-0,78	-1,21	0,11	-0,88	0,67	0,09	0,71
ALL	2A	-0,10	0,01	-0,88	-1,28	0,05	-0,92	0,54	0,14	0,54
	2D	-0,07	0,02	-0,52	-1,23	0,07	-0,94	-0,05	0,11	-0,04
	2E	-0,08	0,01	-0,72	-1,29	0,12	-0,84	0,14	0,15	0,19
	2F	-0,10	0,01	-0,80	-1,91	0,08	-0,96	0,49	0,13	0,48
	All regions	-0,08	0,01	-0,94	-1,16	0,07	-0,96	-0,09	0,11	-0,12

P-value
> 0,05
< 0,05 & > 0,01
< 0,01

Figure S11. Spearman's rank correlations, slopes, and p-value for three parameters: sea ice concentration (SIC), Lower-Tropospheric Stability (LTS), and surface temperature (Surf_Temp). Simple regressions are applied to the normalized data to compare the slopes. Correlations are made for low-level (between clutter height and 3000 m above ground level) MPCs, USLCs, ice clouds, and total clouds.

Section S1

For the first 4 years of data (2007-2010), the CloudSat satellite operated normally, sampling the atmosphere 10 to 15 seconds ahead of CALIPSO. In 2011, a battery problem on CloudSat led to a loss of synchronization with CALIPSO and operational problems with the CPR radar. CloudSat resumed joint observations with CALIPSO in 2012. However, technical problems necessitated the adoption of a new mode (Daylight Only Operations) for data from 2013 to 2016 (Braun et al., 2019; Listowski et al., 2019). During this second measurement period, CloudSat was only able to take atmospheric measurements during the daytime part of its orbit, for about 60 out of the 99 minutes of full orbit. As a result, about 40% of the scientific data could not be exploited (Kotarba, 2022). This missing data concerns the nighttime period. Cloud climatology conducted using CloudSat data after 2012 shows a bias, particularly over the oceans (Noel et al., 2018). Data availability for this study is shown in Figure S4b.

A comparison of the average number of observations per grid cell as a function of latitude highlights the differences between seasons and periods (Fig. S4a). Overall, the number of observations is reduced by 30% for low-latitude meshes (latitude $<$ 66-68°) between the two periods due to daylight-only operation in 2013-2016, especially for winter and autumn. For summer and spring, this difference is much less pronounced, due to the polar day during these seasons. For high-latitude grids (latitude $>$ 76-78°) the difference is very small in spring, summer, and autumn. Winter is the season with the largest discrepancy in the number of observations, especially for high-latitude meshes (latitude $>$ 76-78°) due to the polar night. The last mesh (80-82°) loses up to 80% of the number of observations between the two periods. During the second period, observations are significantly reduced (especially in winter) for these meshes and, more generally, for high-latitude regions.

Figure S4c compares the average occurrences over the two periods (2007-2010 and 2013-2016). A comparison between seasons shows that for total clouds, there seems to be no significant difference between the two periods. For example, there is a slight increase in average occurrences in winter for the period 2013-2016 (42.3% vs. 43.7%). This increase could be due both to the instrument malfunction and to the greater presence of clouds. The comparison for MPCs shows a slightly different behavior, with a seasonal decrease in occurrences over the period 2013-2016 (+1% for MAM vs. -2% for SON). Figure S5 shows a comparison of occurrences for the period 2007-2010 (satellite instruments operational) using 2 operating modes (day only and day/night) for 3 high-latitude regions (affected by polar night). In terms of occurrences, the greatest differences are observed in December and January. However, these differences are larger for region Svalbard (2A) (Fig. S5) than for regions Eastern Arctic (2F) or Northern Canada/Nunavut (2D). The maximum difference for the Svalbard region (2A) is observed in January, with an average difference of 15% for all low-level clouds. In contrast, Fig. S5 shows an underestimation of occurrences for the 2D region in early winter (November and December), but this remains below 5%. As in Noel et al. (2018), it seems that the strongest anomalies are found over oceanic areas. Comparisons for other cloud types show maximum differences of 5% average occurrence during January. These differences appear to be consistently positive for daytime measurements, which means that there may be slight overestimation of cloud occurrences due to the CloudSat Daylight Only Operations mode over the period 2013-2016 for high-latitude regions during December and January.

Section S2

Calculating cloud occurrences involves statistical uncertainties. All the different statistical parameters calculated for this study are shown in Figure S8. They are calculated from each grid cell (1°x1°) averaged

over 1 week of measurements, resulting in a study area represented by approximately 3,300,000 points. The medians are not the same as those shown in the main figures; they are not calculated on the same time scales (monthly/annual). For the whole area, the average cloud occurrence is 73%, with a standard deviation of 30%. The standard deviation obtained (Gaussian distribution hypothesis) for the different regions of the study area varies between 27 and 32%. In this study, the Wilcoxon-Mann-Whitney and Kolmogorov-Smirnov tests (not shown here) are used to evaluate the statistical significance of the observed disparities between regional cloud occurrences. Statistical analysis indicates that the cloud occurrence distribution does not align with the normal hypothesis and that these distributions vary significantly between the different regions that are studied. Therefore, we choose to use the median cloud occurrence and the Median Absolute Deviation (MAD), which are more robust parameters to characterize non-Gaussian samples.

References

Bazantay, C., Jourdan, O., Mioche, G., Uitz, J., Dziduch, A., Delanoë, J., Cazenave, Q., Sauzède, R., Protat, A., and Sellegri, K.: Relating Ocean Biogeochemistry and Low-Level Cloud Properties Over the Southern Oceans, Geophysical Research Letters, 51, e2024GL108 309, https://doi.org/10.1029/2024GL108309, 2024.

Braun, B. M., Sweetser, T. H., Graham, C., and Bartsch, J.: CloudSat's A-Train Exit and the Formation of the C-Train: An Orbital Dynamics Perspective, in: 2019 IEEE Aerospace Conference, pp. 1–10, IEEE, Big Sky, MT, USA, ISBN 978-1-5386-6854-2, https://doi.org/10.1109/AERO.2019.8741958, 2019.

Kotarba, A. Z.: Errors in global cloud climatology due to transect sampling with the CALIPSO satellite lidar mission, Atmospheric Research, 279, 106 379, https://doi.org/10.1016/j.atmosres.2022.106379, 2022.

Listowski, C., Delanoë, J., Kirchgaessner, A., Lachlan-Cope, T., and King, J.: Antarctic clouds, supercooled liquid water and mixed phase, investigated with DARDAR: geographical and seasonal variations, Atmos. Chem. Phys., 19, 6771–6808, https://doi.org/10.5194/acp-19-6771-2019, 2019.

Noel, V., Chepfer, H., Chiriaco, M., and Yorks, J.: The diurnal cycle of cloud profiles over land and ocean between 51° S and 51° N, seen by the CATS spaceborne lidar from the International Space Station, Atmos. Chem. Phys., 18, 9457–9473, https://doi.org/10.5194/acp-18-9457-2018, 2018.